TIME DEPENDENCE OF MICROSECOND INTENSE ELECTRON BEAM TRANSPORT IN GASES

R. F. Lucey, Jr., R. M. Gilgenbach, J. E. Tucker, M. L. Brake, C. L. Enloe and T. E. Repetti
Intense Energy Beam Interaction Laboratory
Nuclear Engineering Department
The University of Michigan
Ann Arbor, MI 48109

SUMMARY

We present results of long-pulse (0.5 μs) electron beam propagation in the ion focused regime (IFR). Electron beam parameters are 800 kV with several hundred amperes injected current. For injection into air (from 0.7 mTorr to 75 mTorr) and helium (from 14 mTorr to 227 mTorr) we observe a "time-dependent propagation window" in which efficient (up to100 %) propagation starts at a time comparable to the electron impact ionization time needed to achieve $n_i \sim (1/\gamma^2)n_{eb}$. The transport goes abruptly to zero about 50 - 150 ns after this initial propagation. This is followed by erratic propagation often consisting of numerous narrower pulses 10 - 40 ns wide. In these pulses the transported current can be 100 % of the injected current, but is generally lower. As the fill pressure is increased, there are differences in the propagated beam pulse, which can be summarized as follows:
1) the temporal occurrence of the beam propagation window shifts to earlier times,
2) the propagated beam current has much faster risetimes,
3) a larger portion of the injected beam is propagated.
Similiar results are observed when the electron beam is propagated in helium. However, at a given pressure, the beam transport window occurs at later times and exhibits a slower risetime. These effects are consistent with electron beam-induced ionization. Experiments are being performed to determine if the observed beam instability is due to the ion hose instability or streaming instabilities.

INTRODUCTION

The purpose of these experiments is to extend the understanding of intense electron beam propagation in low-pressure gas to microsecond pulselengths. This pressure regime has been used for the propagation of short pulse beams and is known as the ion focused regime (IFR).[1] In this regime, the net radial force due to the beam self-fields is counteracted by the space charge of ions in a propagation channel. For beams propagating in neutral gas, the head of the beam spreads due to space charge, while simultaneously ionizing the gas by direct impact ionization. Since recombination times are long compared to the beam pulse, this ionization results in an increasing degree of space charge neutralization. Force-free propagation occurs when the ion density is between n_{eb}/γ^2 and n_{eb}.

The process of beam induced ionization continues through the duration of the pulse. This excess ionization could eventually result in the beam-channel system becoming unstable due to the two-stream interaction.[1,2] For these long-pulse beams, the ion hose instability [3,4] could also be present.

EXPERIMENTAL CONFIGURATION

These experiments are performed using the Michigan Electron Long Beam Accelerator (MELBA). This versatile pulse power generator can supply as much as 1 MV for over 1.5 μs, controlled by crowbar timing, into a typical impedance of 100 Ω. These parameters represent power levels to 10 GW and an energy per pulse up to 15 kJ. The generator is a seven-stage Marx generator with an additional ringing reverse-charged stage [5,6] which can compensate the voltage for the usual RC decay of the Marx and the decreasing impedance of a cold cathode diode. The operation of MELBA is described in more detail in Reference 6.

The experimental configuration is shown in Figure 1. A field emission diode is employed with no applied magnetic field. This cathode is 8 cm from the anode plane. The cathode is a flat 2.5 cm diameter aluminum disk with carbon fiber tufts 0.25 cm tall spaced on a 0.5 cm square grid. The anode is constructed of Poco Graphite AXF-5Q with a 2.5 cm diameter aperture. Beyond the anode there is a 3.5 cm long vacuum drift space ending in a 6 μm thick aluminized mylar foil. The aluminization faces the diode. This foil is inserted between two O-ring flanges separating the diode chamber from the interaction chamber. This allows the chamber to be backfilled with gas as required. The diode region is pumped to about 10^{-5} Torr by an oil diffusion pump.

The interaction chamber is a large stainless steel tank covered with 1 cm of lead. A 30 cm long, 39 cm diameter entrance leads to the 90 cm long 75 cm diameter chamber. The large diameter of the chamber minimizes wall effects which have been observed by others. Two side ports and three end ports permit access to the interaction region. Attached to the smaller side port is a turbomolecular pump for evacuating the propagation

CH2387-9/87/0000-0963 $1.00 © IEEE

region. Base pressures of 2 x 10^{-6} Torr are achieved before backfilling with the gas of interest. A pyrex window in the opposite side port allows open shutter photos of the beam-generated channel to be taken.

A skimmer probe is inserted through the large side port . This skimmer probe consists of a small piece of NE-102 scintillator housed in copper tubing and coupled to a photomultiplier tube in the screen room by a quartz fiber-optic cable. The probe uses the wall and lead of the side port to shield it from the X-rays generated by the beam scrape-off in the diode region. It is sensitive to X-rays scattered by the tank walls or generated by electrons which have been stopped directly in the range thick copper walls of the skimmer probe itself. The present position of the probe is sensitive to large excursions of the electron beam from the channel.

A moveable Rogowski coil 17 cm in diameter located 97 cm from the anode is used to detect the net current passing through the loop. This coil has an L/R time constant of 60 ns which may limit its usefulness in some experiments. Located axially beyond the Rogowski coil is a Faraday cup mounted on a 2.5 cm copper tube run through a sliding O-ring seal. The Faraday cup is based on a design used at McDonnell-Douglas.[7] This same copper tube is used to shield the signal cable and pump out the Faraday cup. The electrons entering the Faraday cup collector are filtered in energy by a 12 μm titanium foil.

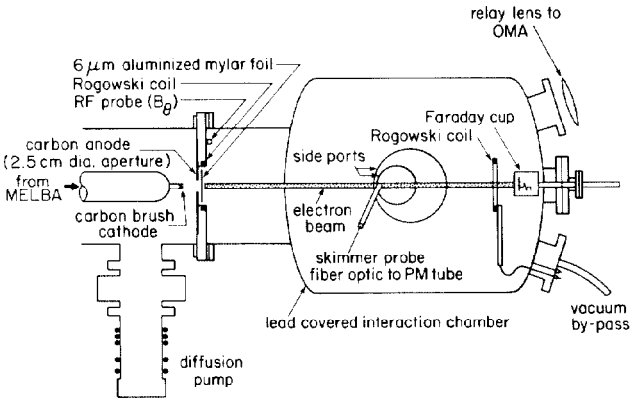

Figure 1. Experimental configuration.

Other diagnostics include RF, microwave and optical detectors. The RF signals are fed either into an array of bandpass filters or into a broadband detector. The filter array separates the signal into frequency regions: 45 MHz to 105 MHz, 138 MHz to 184 MHz, 210 MHz to 265 MHz and 313 MHz to 373 MHz. The microwave emission is studied using an array of successively higher frequency directional couplers and diode detectors. Time-resolved optical emission spectra from the electron beam channel are also measured using a 0.25 m Jarrel-Ash spectrograph with a gated Tracor Northern 1024 channel optical multichannel analyzer (OMA).

RESULTS

These experiments have been undertaken to test the limits of long-pulse electron beam propagation in low-pressure neutral gas. The diode configuration injects approximately 200 amperes at 800 kV for as long as 500 ns into the interaction chamber before crowbarring. In air, the filling pressure is varied from 10^{-3} to 75 mTorr, while for experiments in helium the fill pressure is varied from 1 to 227 mTorr.

Figure 2 presents propagation data for air at 15 mTorr. The injected current turns on when the voltage reaches ~300 kV. After about 200 ns a large increase occurs in the injected current until the voltage pulse is terminated by the crowbar switch. The current jump is accompanied by an large RF signal which then decays away with the time constant of the diode detector. It should be noted that a net current reversal occurs during the rapid rise of the injected current. Transported current is zero until about 100 ns after the start of injected current. At the spike in the transported current the propagation efficiency (I_{tr}/I_{inj}) is approximately 100 %.

After about 100 ns of efficient propagation, the transported current decreases abruptly to zero. This is followed by a series of short (10 ns to 40 ns) spikes which propagate with lower transport efficiency (35 % to 50 %). One can compare the 100 ns turn-on time for beam transport of the first spike to the time required for the electron beam to ionize the background gas to the IFR condition: $f_e \approx 1/\gamma^2$. For 15 mTorr of air and assuming a uniform injected beam radius the IFR condition should be reached after about 20 ns. The fact that the experiment required 100 ns is probably a consequence of the fact that the electron beam radius is very large before significant charge neutralization has taken place.

The skimmer probe trace closely follows the voltage trace indicating that at no time did the electron beam directly reach the probe. This is in contrast to the data presented for helium.

Assuming that $f_e \approx 1/\gamma^2$ during the first spike of efficient propagation, one expects propagation (at $f_e < 1$) to be free from streaming instabilities for a 100 ns period. This agrees with the observed pulselength of the first transported spike. Another possible explanation for the loss of beam propagation and erratic transport behavior at late times is the ion hose instability. Using the scaling from Reference 4 we expect the frequency of the ion hose instability to be approximately 10 MHz. Therefore, the "period" of the spikes of transported current are in qualitative agreement with the period of the ion hose instability. Additionally, Kammash has estimated the growth time for the ion hose instability to be in the neighborhood of 100 ns.

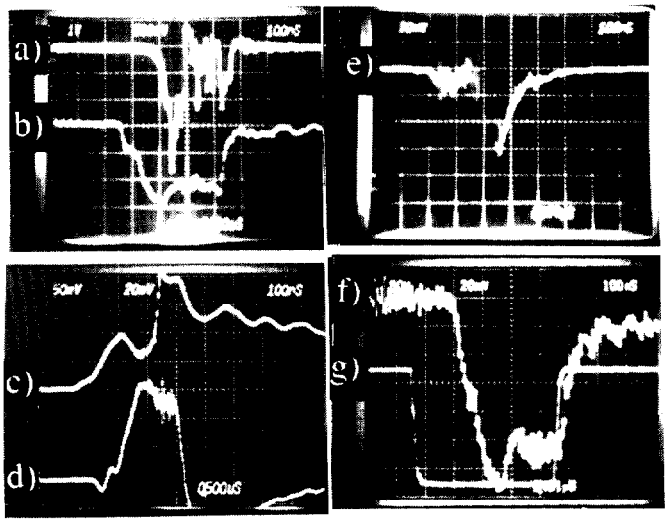

Figure 2. Experimental data (air at 15 mTorr): a) Faraday cup at 102 cm (42 A/div), b) voltage (360 kV/div), c) injected current (112 A/div), d) net current at 97 cm (40 A/div), e) broadband RF, f) skimmer probe, g) OMA gate pulse. Time scale 100 ns/div.

Figure 3 presents propagation data for helium at 227 mTorr. Again, the injected current turns on when the voltage reaches ~300 kV and follows the voltage pulse. The injected current begins to rapidly increase after 270 ns accompanied by an increased RF level. The injected current then fluctuates after the crowbar is fired in a series of broad peaks. An increase in the RF level is associated with each of these peaks.

The transported current shows a turn-on of about 100 ns after the start of the injected current. The propagated current reaches 100 % of the injected current in approximately 80 ns after turn-on, and decays to zero in about 100 ns. For this case, there is a series of highly efficient spikes of transported beam current superimposed on the decaying transported beam pulse.

The lack of transported current late in the voltage pulse was accompanied by a marked increase in the skimmer probe signal, indicating the presence of beam current at large radii. The net current Rogowski signal goes negative after the last spike of current is measured by the Faraday cup. These indicate a gross disruption of the beam.

CONCLUSION

We have presented data which establishes the time dependence of the propagation window for IFR propagation in air and helium. This data is consistent with the creation of an ion channel of sufficient density to neutralize the net radial force of the electron beam. For all pressures the temporal window for efficient propagation is

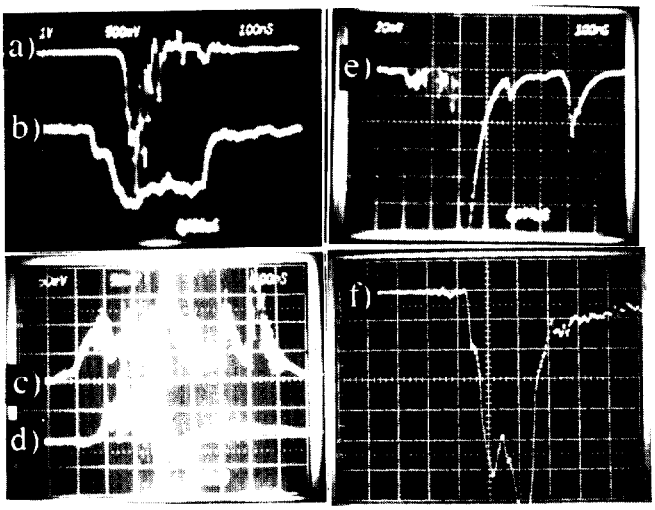

Figure 3. Experimental data (helium at 227 mTorr): a) Faraday cup at 102 cm (42 A/div), b) voltage (360 kV/div), c) injected current (112 A/div), d) net current at 97 cm (101 A/div), e) broadband RF, all at 100 ns/div, f) skimmer probe at 200 ns/div.

about 100 ns. Instabilities at later times result in erratic propagation. Experiments are underway to determine whether these instabilities are due to the ion hose instability or streaming instabilities.

ACKNOWLEDGEMENTS

This research was sponsored by the ONR, NSF and SDIO-IST.

REFERENCES

1. K. W. Struve, E. J. Lauer, and F. W. Chambers, in *Proceedings of the Fifth International Conference on High-Power Particle Beams*, 1983, edited by R. J. Briggs and A. J. Toepfer, CONF-830911, p. 408.

2. E. P. Lee, F. W. Chambers, L. L. Lodestro, S. S. Yu, in *Proceedings of the 2nd International Topical Conference on High Power Electron and Ion Beam Research and Technology*, 1977, vol 1, p 318.

3. H. L. Buchanan, Phys. Fluids, **30**, 221 (1987).

4. K. T. Nguyen, R. F. Schneider, J. R. Smith, and H. S. Uhm, Appl. Phys. Lett., **50**, 239 (1987).

5. E. A. Abramyan, E. N. Efimov, and G. D. Kuleshov, in *Proceedings of the 2nd International Topical Conference on High Power Electron and Ion Beam Research and Technology*, 1977, vol 2, p 755.

6. R. M. Gilgenbach *et. al.*, Invited Paper in *Proceedings of the Fifth IEEE Pulsed Power Conference*, 1985, IEEE Catalog Number 85 C 2121-2, p. 126.

7. M. A. Greenspan and R. E. Juhala, J. Appl. Phys., **57**, 67 (1985).